ISBN: 978-3-95450-231-8 ISSN: 2673-5490 doi: 10.18429/JACoW-IPAC2023-THPM024

LASER POWDER BED FUSION OF CuCrZr FOR NUCLEAR FUSION ACCELERATION COMPONENTS*

M. Bonesso†, V. Candela#,1, S. Candela[1], R. Dima, G. Favero[1], P. Rebesan, A. Pepato Istituto Nazionale di Fisica Nucleare – Padua Division, Padova, Italy
P. Agostinetti Consorzio RFX, Padova, Italy
[1]also at University of Padova, Padova, Italy

Abstract

Copper and copper alloys are widely used in the Nuclear Fusion field for their outstanding characteristics, especially in terms of thermal and electrical conductivities. CuCrZr is peculiarly suitable and well-known in High Energy applications because it combines good conductivity and good mechanical properties. Moreover, the material properties can be tuned with thermal treatments to fit the application requirements even more. Additive manufacturing is then a revolutionizing process that permits the creation of geometrically optimized components. This near-net-shape process allows producing seamless parts reducing material waste and saving time. We investigate the application of the Laser Powder Bed Fusion technology to produce the acceleration grids of a Neutral Beam Injector. In this work, the authors analyzed different CuCrZr powders and investigated the material properties obtained after the printing parameters optimization, in as-built conditions and after different heat treatments. The high density and high mechanical and thermal properties allowed us to proceed with the creation of the first prototypes of the acceleration components.

INTRODUCTION

Printing commercially pure copper can be very tricky if the Laser Powder Bed Fusion (LPBF) Technology is employed. The main reasons are the high reflectivity (especially within the IR range) and the high thermal conductivity. Both these properties reduce the amount of energy available for melting, leading to high porosity and low mechanical and thermal properties [1].

To overcome the low energy issue, two prominent options can be discovered in the literature: increasing the laser power up to 1 kW or using a green laser source [2]. These methods for printing pure copper, however, are incompatible with commercially available LPBF machines, which have a modest laser power (400W max) and a laser wavelength of roughly 1080 nm.

*This work has been carried out within the framework of the EUROfusion Consortium, funded by the European Union via the Euratom Research and Training Programme (Grant Agreement No 101052200 - EUROfusion). Views and opinions expressed are however those of the author(s) only and do not necessarily reflect those of the European Union or the European Commission. Neither the European Union nor the European Commission can be held responsible for them.
† massimiliano.bonesso@pd.infn.it
# valentina.candela@pd.infn.it

Because of their lower reflectance and heat conductivity, copper alloys have been shown to be more printable than pure copper. The primary attribute of the CuCrZr alloy is its outstanding mechanical properties while keeping high conductivity. As a result, in high thermal conductivity applications, the CuCrZr alloy is a suitable pure copper replacement.

This research work presents the tuning of process parameters of an EOS M280 LPBF machine; two batches of CuCrZr powder having different Particle Size Distributions (PSD). The tuning of the process parameters was focused on achieving the lowest porosity on the printed parts.

Printed parts have been heat-treated at different times and temperatures and the micro hardness and thermal conductivity have been measured.

MATERIALS AND METHODS

All of the specimens were produced using an EOSINT M280 powder bed machine coupled with a 400W ytterbium fibre laser. Nitrogen gas was employed as a protective gas during the production process, and the oxygen concentration was controlled (<0.2%).

Two batched of CuCrZr powder have been tested. Both batches have been gas atomized and the particles had a spherical morphology. Figure 1 shows images of the particles obtained with a Scanning Electron Microscope (SEM).

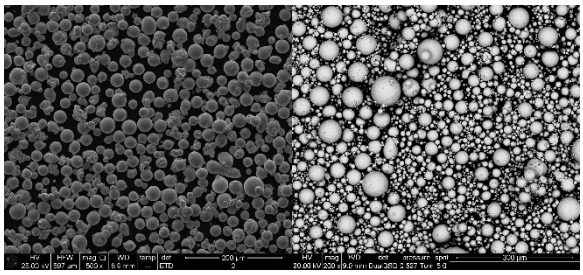

Figure 1: SEM images of Powder A (left) and Powder B (right).

The main difference between the powders is the PSD, the D values of the two powders are reported in Table 1.

Table 1: Particle Size Distribution of the CuCrZr Powders

Powder	D10 [µm]	D50 [µm]	D90 [µm]
A	19	27	40
B	14	33	60

ISBN: 978-3-95450-231-8 ISSN: 2673-5490 doi: 10.18429/JACoW-IPAC2023-THPM024

Compared to powder A, powder B presented a broader distribution, as the diameter of the particles lies in the range between 14 μm and 60 μm.

The main process parameters that have been studied were the laser power, the laser scan speed, and the hatching distance (the distance between two adjacent scan tracks). The layer thickness also strongly influences the quality of the printed parts [3]. For powder A it was kept constant at the minimum value of 20 μm, as smaller layers require less energy to melt. Since powder B presented bigger particles, it was not possible to maintain the same thickness and a layer of 30 μm was selected.

The density of the samples was determined using the Archimedes technique in accordance with ASTM B311-17. The porosity was then estimated by comparing the sample density to the density of bulk CuCrZr (8.89 g/cm^3).

The microstructure of the printed parts has been observed by means of an optical microscope on polished surfaces etched using a solution of 1 ml HCl, 2.5 g FeCl3, and 100 ml EtOH.

Thermal conductivity was measured using an experimental approach based on the physical basis of Fourier law. The ASTM E12225-20 standard was followed.

Micro-hardness measurements were performed on the samples using a micro-hardness tester with a 300 g load.

RESULTS AND DISCUSSION

Parameter Optimization

Nearly full dense samples have been manufactured using both powders. With powder A, it was found that densities over 99.5% are reached when using the highest laser power possible (370 W) and a laser scan speed of up to 800 mm/s. The optimal hatching distance was 90 μm.

Relative densities over 99% were obtained using powder B, slightly lower if compared to powder A. In this case, the hatching distance that maintained a porosity of less than 1% was 70 μm. The melt pools need to overlap more due to the higher layer thickness. The laser scan speed was also reduced to 650 mm/s (maximum value). The build rate of both powders however is very similar, as the decrease in laser scan speed and hatching distance is compensated by the higher layer thickness.

As-Built Microstructure Characterization

Figure 2 shows the microstructure of the highest-density as-built components for powder A and powder B. The XZ plane (parallel to the building direction) has been observed.

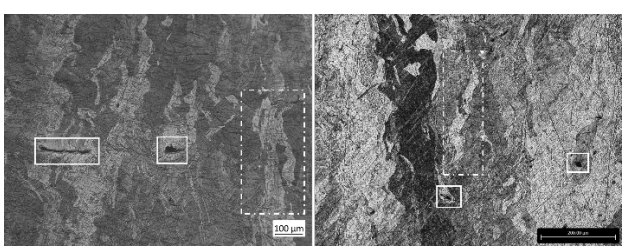

Figure 2: Microstructure of the XZ plane of the as-built components of powder A (left) and powder B (right). The dashed rectangular highlights the columnar grains, and the continuous line highlights the lack-of-fusion pores.

In both cases, the traditional columnar microstructure is observed. The microstructure is a consequence of the building process. The grains grow towards the highest thermal gradient and in the case of the LPBF process, it is the centre of the molten pool (parallel to the building direction). Lack-of-fusion porosities were also observed. As seen in Fig. 2, in some parts of the layer the melt pool fails to remelt the underlying layer, generating a porosity whose main axis is oriented perpendicular to the building direction.

Heat Treatments

The CuCrZr alloy is age-hardenable. To obtain the required mechanical and physical properties the material needs two heat treatments: a solution anneal heat treatment followed by an age-hardening heat treatment. The solution anneal heat treatment consists in maintaining the material at high temperatures (around 900°C) for a short time followed by water cooling, while the age hardening heat treatment consists in maintaining the material at an intermediate temperature (between 300 °C and 600 °C) for longer times followed by slow cooling in air. The LPBF process could be approximated to a solubilization heat treatment since the process generates high cooling rates [4]. Therefore it is possible to directly age the as-built parts without the solubilisation heat treatment [5].

Two heat treatments have been performed. The powder A samples have been age hardened for 300 minutes at 580 °C, while powder B samples have been age hardened for 60 minutes at 550 °C.

Microhardness and Thermal Conductivity

The microhardness results are summarized in Table 2.

Table 2: Micro-Hardness of LPBF CuCrZr Samples

	Powder A	**Powder B**
As-built	92 HV0.3	83 HV0.3
Heat-treated	133 HV0.3	165 HV0.3

In the as-built condition, the powder A sample shows a higher hardness, 92 HV0.3 versus the 83 HV0.3 obtained with the powder B sample. The reason for this divergence could be attributed to the higher porosity level of the powder B sample. Under the applied force, the pores inside the material collapse, resulting in a decrease in micro-hardness [6].

Heat treating the parts leads to an increase in hardness. The age-hardening heat treatments precipitate the Cr and Zr that were previously solubilized into the copper matrix. The presence of particles in the copper matrix improves mechanical properties primarily through the Orowan strengthening process [7]. The heat-treated powder B sample shows the highest hardness of 165 HV0.3, while the heat-treated powder A sample had a much lower hardness of 133 HV0.3. In this case, the difference in hardness is due

ISBN: 978-3-95450-231-8 ISSN: 2673-5490 doi: 10.18429/JACoW-IPAC2023-THPM024

to the parameters of the heat treatments. The powder A sample is probably over-aged. When heat is treated at too high temperatures or for a too long time, the materials form fewer precipitates with bigger dimensions.

The heat treatments also affect the thermal conductivity of the material. Once out of the solution Cr and Zr debase the thermal conductivity to a lower level.

Indeed, the thermal conductivity of the as-built components is low. Both powder A and B samples had a thermal conductivity of ~100 W/(m*K). The age-hardening heat treatment drastically increased the conductivity of the material, 320 W/(m*K) for powder A and 315 W/(m*K). The difference in thermal conductivity is neglectable as the experimental apparatus had an uncertainty of 5%.

The heat treatment at 550 °C for 60 minutes is better, as it leads to higher mechanical properties while still generating a high thermal conductivity.

Prototyping

The good results in terms of relative density, hardness and thermal conductivity have permitted the realization of a reduced-dimension Hyperlens grid, shown in Fig. 3.

The part has been successfully manufactured using powder B, with only a slight overheating on the top section. Currently, the part needs to be machined and then several tests will be performed.

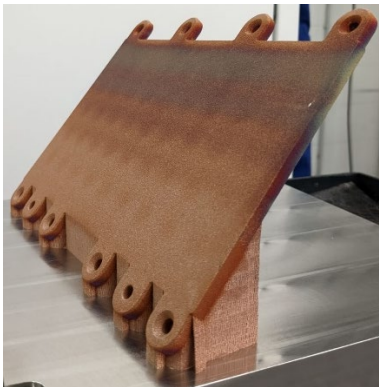

Figure 3: Hyperlens grid manufactured at the Padova division of INFN

CONCLUSIONS

This research work has demonstrated that it is possible to obtain near fully dense CuCrZr components while using a low-power LPBF machine.

Two powders with different PSD have been tested and in both cases, relative densities above 99% were reached. The microstructure of the parts is the standard columnar microstructure of LPBF components and few lack-of-fusion defects were observed.

Two heat treatments have been tested, one at 580 °C for 300 minutes and one at 550 °C for 60 minutes. The results of the microhardness and the thermal conductivity measurements indicate that better results are obtained after heat treating the part for a shor time at a lower temperature. In fact, with this heat treatment, the parts have a much higher hardness of 165 HV0.3 (versus 133 HV0.3) and the same thermal conductivity of ~320 W/(m*K).

Finally, thanks to this characterization it was possible to successfully manufacture a scaled version of a Hyperlens Grid.

ACKNOWLEDGMENTS

This work has been carried out within the framework of the EUROfusion Consortium, funded by the European Union via the Euratom Research and Training Programme (Grant Agreement No 101052200 - EUROfusion). Views and opinions expressed are however those of the author(s) only and do not necessarily reflect those of the European Union or the European Commission. Neither the European Union nor the European Commission can be held responsible for them.

REFERENCES

[1] M. Bonesso *et al.*, “Effect of Particle Size Distribution on Laser Powder Bed Fusion Manufacturability of Copper”, *BHM Bergund Hüttenmännische Monatshefte*, vol. 166, pp. 256–262, 2021.

[2] M. Roccetti Campagnoli, M. Galati, and A. Saboori, “On the processability of copper components via powder-based additive manufacturing processes: Potentials, challenges and feasible solutions”, *J. Manuf. Process.*, vol. 72, pp. 320–337, 2021.

[3] M. F. Zaeh and G. Branner, “Investigations on residual stresses and deformations in selective laser melting”, *Prod. Eng.*, vol. 4, pp. 35–45, 2010.

[4] P. A. Hooper, “Melt pool temperature and cooling rates in laser powder bed fusion”, *Addit. Manuf.*, vol. 22, pp. 548–559, 2018.

[5] C. Wallis and B. Buchmayr, “Effect of heat treatments on microstructure and properties of CuCrZr produced by laser-powder bed fusion”, *Mater. Sci. Eng. A*, vol. 744, pp. 215–223, 2019.

[6] J. A. Cherry, H. M. Davies, S. Mehmood, N. P. Lavery, S. G. R. Brown, and J. Sienz, “Investigation into the effect of process parameters on microstructural and physical properties of 316L stainless steel parts by selective laser melting”, *Int. J. Adv. Manuf. Technol.*, vol. 76, pp. 869–879, 2015.

[7] S. Uchida *et al.*, “Microstructures and electrical and mechanical properties of Cu-Cr alloys fabricated by selective laser melting”, *Mater. Des.*, vol. 175, p. 107815, 2019.